Supplementary Methods:

Reagents

Pertussis toxin, prostaglandin (PG) E_2 (PGE_2), H-89, Y-27632 (hydrochloride), Latrunculin B, C3 transferase, sulprostone and Wortmannin were obtained from Cayman Chemical Company. SU5416, Monocrotaline (MCT) and L-798106 were purchased from Sigma Chemical Company (Sigma-Aldrich).

Hemodynamic measurement

Mice or rats were anaesthetized by intraperitoneal injection with 10% chloral hydrate (4 μL/g body weight). After a left parasternal incision, small parts of the ribs were carefully resected, a 1.4-F micro-tip pressure transducer catheter (Millar Instruments) was inserted directly into the right ventricle, and right ventricular pressure was continuously monitored for 5 min using a PowerLab data acquisition system (ADInstruments).

Histological analysis

After hemodynamic measurements, the pulmonary circulation was flushed with chilled PBS, and the heart and lungs were removed. The right ventricle (RV) was carefully dissected from the heart and weighed. Right ventricular hypertrophy was assessed by normalizing the weight of the RV to the weight of the left ventricle plus septum (RV/LV+S).

The left lungs were placed in liquid nitrogen for preparation of homogenates, and the lower lobes of the right lungs were fixed with 4% PFA for 24 h. After paraffin embedding and sectioning, the slides (5-μm thickness) were stained with hematoxylin and eosin (H&E) for morphological analysis. Pulmonary vascular remodeling was quantified by accessing the medial wall thickness and the percentage of muscularization. To determine the degree of medial wall thickness, 15-20 muscular arteries categorized 20-50μm and 51-100μm in diameter from each lung were randomly outlined by an observer blinded to mouse genotype or pharmacological treatment. The degree of medial wall thickness, expressed as a ratio of medial area to cross sectional area (i.e., Media/CSA) (1, 2), were analyzed using imageJ. To access the degree of muscularization, 40 to 60 intraacinar vessels at a size between 20 to 50μm in each mouse were categorized as nonmuscular (i.e., no apparent muscle), partially muscular (i.e., with only a crescent of muscle), or muscular (i.e., with a complete medial coat of muscle), as previously reported (3). The degree of muscularization was expressed as ratio of non-, partially-, fully muscular vessels to the number of total vessels.

Masson's trichrome staining was performed following the munufactuer's

instructions (Sigma-Aldrich).

Cell culture

Primary mouse pulmonary artery (PA) smooth muscle cells (PASMCs) were cultured from 6–8 week old mice as described before. In brief, proximal PAs from the lung lobe were aseptically excised and placed in DMEM (Gibco) at room temperature. Adhering fat and connective tissues were carefully removed under a dissecting microscope, and the luminal surface was scraped with forceps to remove endothelial cells. The dissected media of the vessels was then cut into small pieces (1–2 mm^2) and transferred into cell-culture flasks. The cells were cultured in DMEM/F-12 (Gibco) supplemented with 100 U/mL penicillin, 0.1 mg/mL streptomycin, 2 mM L-glutamine, and 20% FBS and were grown in a humidified incubator (Thermo Scientific) at 37°C in 5% CO_2/95% air. After one week, the PASMCs were transferred into new cell-culture flasks. Cultured PASMCs were used between passages 3 and 6. The smooth muscle cells were identified by positive immune staining with antibodies against α-smooth muscle actin (Sigma-Aldrich). Human PASMCs were purchased from ScienCell Research Laboratories. For hypoxia exposure in vitro, PASMCs seeded in culture dishes were subjected to a hermetic tank that contained 1% O_2/5% CO_2 (4).

To culture lung endothelial cells, lungs from VSMC- and EC-specific EP3 knockout mice were isolated and digested with 600 U/mL collagenase type Ⅰ(Worthinton) and DNase Ⅰ(60 U/mL, Worthington) in DPBS (Life Technologies) at 37°C for 30 min, added with anti-mouse CD31 and CD102 antibodies and based on magnetic bead separation. CD31- and CD102- positive cells were used for gene expression analysis (5).

RNA extraction and real-time PCR

Total RNA from lung homogenates, primary PASMCs and human distal PAs and mouse proximal PAs was extracted by use of Trizol reagent (Invitrogen), according to the manufacturer's protocols. Briefly, total RNA (1 μg) was reverse-transcribed to cDNA by use of Reverse Transcription Reagent kits (Transgene), according to the manufacturer's instructions. The resulting cDNA was amplified with 40 PCR cycles by real-time PCR. Each sample was analyzed in triplicate and was normalized to a reference RNA within the sample. Quantitative PCR products were confirmed by a single band of expected size on a 2% agarose gel. The primer sequences for PCR are summarized in **Supplementary Table 1**(mouse) and **Table 2** (human) .

Western blotting

Concentrations of proteins extracted from lung homogenates or PASMCs were

determined using a Pierce BCA Protein Assay Kit (Pierce, Rockford, IL). Membrane proteins were extracted using the Plasma Membrane Protein Extraction Kit (BioVision; K268-50). The cytosol fractions were collected just after first centrifugation at 10,000 x g for 30 min. Equal quantities of proteins were denatured and resolved by 10% SDS-PAGE, transferred to nitrocellulose membranes, incubated with 5% skimmed milk for 1–1.5 h, and then incubated with primary antibodies overnight at 4°C. Primary antibodies were diluted as follows: collagen-1 (NBP1-30054; Novus), fibronectin (1574-1; Epitomics), tenascin-C (311B-1, Epitomics), phospho-Smad2 (AB3849; Millipore), total Smad2 (5339; Cell Signaling Technology), phospho-Smad3 (9520; Cell Signaling Technology), total Smad3 (9523; Cell Signaling Technology), Smad4 (9515; Cell Signaling Technology), membrane type-1 (MT1)-MMP (AB8221; Millipore), Lyn (ab137338; Abcam), $G\alpha_{12}$ (sc-409; Santa Cruz), $G\alpha_{13}$ (sc-410; Santa Cruz) and GAPDH (5174; Cell Signaling Technology). The membranes were then conjugated with a horseradish peroxidase (HRP)-labeled secondary antibody in blocking buffer for 2 h at room temperature. Blots were developed using an enhanced chemiluminescence reagent (Thermo Scientific), followed by densitometric quantification using ImageJ.

Hybridization in situ

RNA hybridization in situ was performed with a commercial kit (Boster Company), according to the manufacturer's instructions. Briefly, lung tissues were cryoprotected in 30% sucrose/ diethylpyrocarbonate (DEPC)-PBS overnight at 4℃ after fixation with 4% paraformaldehyde (PFA), then embedded in OCT and cut to 12 μm sections at -20℃ using a cryostat. Tissue sections were warmed to room temperature (RT) for 1 h then incubated with digoxin-labeled RNA probes (5'oligo TGCTGGGCGTGGGCCGCTACA; 3'oligo ACCCAGGGATCCAAGATCTGG) (6) with coverslips on top of the slides. The slides were then placed in a sealable plastic box containing 2 sheets of Whatman paper wet with 5% formamide and incubated at 65℃ overnight. The coverslips were carefully removed the next day and the sections were washed with 2×SSC at 65℃ for 15 min and 0.5×SSC for 5 min, then biotin-streptavidin-conjugated mouse anti-digoxin antibody was added and incubated at 37℃ for 2 h. After 3 washes, the slides were incubated with streptavidin biotin complex at 37℃for 30 min. Then, biotinylated peroxidase was added and incubated for an additional 30 min and brown color was developed by addition of diaminobenzidine (DAB) after extensive washing.

Immunostaining

For immunofluorescence staining, deparaffinized and dehydrated tissue sections (5 μm) were blocked by diluted normal serum to prevent nonspecific binding. Tissues

were incubated with primary antibodies against fibronectin (1:300; Epitomics), collagen 1 (NBP1-30054; Novus), tenascin-C (311B-1; Millipore), phospho-smad2 (AB3849; Millipore), CD11b (550282; BD Pharmingen), CD68 (MCA1957; AbD Serotec), PCNA (13110; Cell Signaling Technology) and FITC-conjugated α-smooth muscle actin (F3777Sigma-Aldrich) overnight at 4°C. After incubation with Alexa Fluor 594-conjugated secondary antibodies (ab150092; Abcam), slides were then counter-stained with DAPI, sealed with antifade reagent, and were visualized using a laser scanning confocal microscope (Carl Zeiss).

To detect actin filaments, PASMCs grown on glass coverslips were stimulated with 1% hypoxia with or without pretreatment with 10 nM Latrunculin B, 0.25 μg/mL C3 transferase, or Y-27632 10 μM, washed in PBS, fixed in 4% PFA, blocked in PBS containing 1% BSA, and incubated with rhodamine-conjugated phalloidin (Invitrogen) for 1 h.

PG extraction and analysis

Lung homogenates were centrifuged, and supernatant (500 μL) was used for PG extraction after protein quantification. Internal standard (2 μL) was added to the sample with 40 μL citric acid (1 M) and 5 μL of 10% butylated hydroxytoluene, and then the sample was vigorously shaken with 1 mL solvent (normal hexane: ethyl acetate, 1:1) for 1 min. The supernatant organic phase was collected after centrifugation (6000 g/min) for 10 min, dried by a gentle stream of nitrogen, dissolved in 100 μL of 10% acetonitrile in water, and passed through small centrifugal filters with a 0.2 μm nylon membrane before analysis by LC/MS/MS. PG production was normalized to total protein.

Rho GTPase activity assay

PASMCs from *EP3* KO mice transfected with *EP3A/B* or control empty vectors were grown to confluence on 15-cm^2 dishes, serum-starved for 20 h with or without hypoxia stimuli, and then incubated with PGE_2 (10 μmol/L; Cayman Chemical) for 5 min at 37°C. Cells were washed with cold PBS and then harvested in ice-cold lysis buffer (containing 1% protease inhibitor), which was specifically provided by the RhoA Activation Assay kits (Cell Biolabs). Active RhoA was determined according to the manufacturer's protocol.

Gelatin zymography

Conditioned culture media were prepared in a standard, non-reducing 2× loading buffer for SDS-PAGE. Gelatin liquor (1%, 0.5 mL) was embedded in the separation gel (10%, 5 mL) during preparation of the acrylamide gel. Following electrophoresis, the SDS was removed from the gel by washing 3 times for 25 min with buffered 2.5%

Triton X-100 solution, followed by incubation in an appropriate digestion buffer (pH 7.6, 50 mM Tris-HCl, 10 mM $CaCl_2$, and 5 mM NaCl) for 42 h at 37°C. The gel was subsequently stained with Coomassie Brilliant Blue, and areas of digestion appeared as white bands against a blue background, which is proportionate to MMP activity.

Cell proliferation assay

Cell proliferation analysis was perfomed using a cell counting kit (CCK)-8 (Beyotime) according to the manufacturer's instructions. Cell suspension (100 μL /well) was pre-incubated in a 96-well plate in a humidified incubator. CCK-8 solution (10 μL) was added to each well of the plate and then incubated for 3 hours in the incubator for measurement of absorbance at 450 nm using a microplate reader.

Globular-actin (G-actin) versus F-actin quantification

The ratio of F- to G-actin in murine PASMCs was determined using an in vivo F/G-Actin Assay kit (Cytoskeleton, Inc.) according to the manufacturer's instructions.. Briefly, PASMC lysates were created in the supplied lysis buffer and centrifuged for 10 min. To separate F- and G-actin contained in the supernatant, samples were centrifuged again at 37°C for 1 h at 100,000 × g. The pellet containing F-actin was resuspended in ice-cold supplied depolymerization buffer for dissociation. Equal volumes of the 2 fractions were then analyzed by 12% SDS-PAGE and subsequently by Western blotting using the anti-actin antibody provided.

Overexpression of m*EP3* variants

The mouse *EP3* variant cDNAs were subcloned into pcDNA3.1, and an HA tag was added at the extracellular N-terminus. PASMCs from *EP3* KO mice were transiently transfected with each pcDNA3/*EP3* variant or pcDNA3 empty vector using Lipofectamine 2000 transfection reagent (Invitrogen), according to the manufacturer's protocol.

Gene interference

Small interfering RNA (siRNA) targeting common *EP3* or siRNA specific for each *EP3* variant was transiently transfected into PASMCs grown to about 80% confluence with RNAiFect Transfection Reagent (Qiagen), according to the manufacturer's instructions. A scrambled siRNA was used as a negative control. Sequences of siRNAs are shown in **Supplementary Table 3**.

PASMCs were transiently transfected with short hairpin RNA (Genepharma) targeting $G\alpha_{12}$ and $G\alpha_{13}$, using Lipofectamine 2000 transfection reagent (Invitrogen) according to the manufacturer's protocol. Knockdown efficiency was determined by Western blot analysis 72 h after transfection.

Co-immunoprecipitation

PASMCs were transiently transfected with *EP3*A and *EP3*B variants or empty vector using Lipofectamine 2000 transfection reagent. After 48 h transfection, serum-starved PASMCs were stimulated with PGE_2 for 5 min. Then whole cell lysates (1 mg) were incubated with 5 μg of HA-tag antibody at 4°C for 3 h, followed by incubation with protein A/G agarose (Invitrogen) at 4°C overnight with gentle agitation. After extensive washing, the immune complexes were separated by SDS-PAGE, and the proteins were detected by Western blot analysis with an HA-tag antibody.

References

1. Hameed, A.G., Arnold, N.D., Chamberlain, J., Pickworth, J.A., Paiva, C., Dawson, S., Cross, S., Long, L., Zhao, L., Morrell, N.W., et al. 2012. Inhibition of tumor necrosis factor-related apoptosis-inducing ligand (TRAIL) reverses experimental pulmonary hypertension. *J Exp Med* 209:1919-1935.
2. Ma, W., Han, W., Greer, P.A., Tuder, R.M., Toque, H.A., Wang, K.K., Caldwell, R.W., and Su, Y. 2011. Calpain mediates pulmonary vascular remodeling in rodent models of pulmonary hypertension, and its inhibition attenuates pathologic features of disease. *J Clin Invest* 121:4548-4566.
3. Schermuly, R.T., Dony, E., Ghofrani, H.A., Pullamsetti, S., Savai, R., Roth, M., Sydykov, A., Lai, Y.J., Weissmann, N., Seeger, W., et al. 2005. Reversal of experimental pulmonary hypertension by PDGF inhibition. *J Clin Invest* 115:2811-2821.
4. Weisel, F.C., Kloepping, C., Pichl, A., Sydykov, A., Kojonazarov, B., Wilhelm, J., Roth, M., Ridge, K.M., Igarashi, K., Nishimura, K., et al. 2014. Impact of S-adenosylmethionine decarboxylase 1 on pulmonary vascular remodeling. *Circulation* 129:1510-1523.
5. Yu, Y., Qin, J., Chen, D., Wang, H., Wang, J., and Yu, Y. 2014. Chronic Cardiovascular Disease-Associated Gene Network Analysis in Human Umbilical Vein Endothelial Cells Exposed to 2,3,7,8-Tetrachlorodibenzo-p-dioxin. *Cardiovasc Toxicol*.
6. Hao, C.M., and Breyer, M.D. 2008. Physiological regulation of prostaglandins in the kidney. *Annu Rev Physiol* 70:357-377.

Supplementary Table 1.

Primers for real-time PCR analysis for mouse samples

Gene	Sense	Anti-sense
EP1	TAACGATGGTCACGCGATGG	ATGCAGTAGTGGGCTTAGGG
EP2	GCTCGCCTGCAACATCAGCGTTA	AGCTCGGAGGTCCCACTTTTCCT
EP3	CGCACAGCAACCTGTCAAGTA	CCCCACTAAGTCGGTGGAGC
EP3A	GGATCATGTGTGTGGTGTCC	GCAGAACTTCCGAAGAAGGA
EP3B	TGAACAACCTGAAGTGGACTTTC	ATTCTCAGACCCAGGGAAACAGG
EP3G	TTCGCTGAACCAGATCTTGGATC	TAGACAATGAGATGGCCTGCCCT
EP4	GTGGTGCTCATCTGCTCCATTCC	AGGATGGGGTTCACAGAAGCAAT
FN	GAAGTCGCAAGGAAACAAGC	GCCACCATAAGTCTGGGTCA
COL1A1	CTACTCAGCCGTCTGTG CCT	GAACGGGAATCCATCGGTCAT
COL1A2	CAACTCAGCTCGCCTTCATG	AGGTACGCAATGCTGTTCTTG
Tn-C	GCTTTGTTTGCCCTCACTCC	GGGTCATGTTTAGCCCACTCT
Elastin	CACTGGCACAGGAGTCAAAGC	GGTATAGGGCAGTCCGTAGCC
MMP-2	AATGCCATCCCTGATAACCT	ACTTCACGCTCTTGAGACTTTG
MMP-9	TTTGAGTCCGGCAGACAATC	CCAACCGTCCTTGAAGAAATG
IntegrinA5	GGTGCCATCTCAAATCCTCG	CAACGGGTCTGGCTCTGTAT
Tsp1	GAAATGTGGTGCGTGTCCTC	CGATGTTCTCCGTTGTGATTG
GAPDH	CCCTTATTGACCTCAACTACATGGT	GAGGGGCCATCCACAGTCTTCTG

Supplementary Table 2.

Primers for real-time PCR analysis for human samples

Gene	Sense	Anti-sense
EP1	TAACGATGGTCACGCGATGG	ATGCAGTAGTGGGCTTAGGG
EP2	GCTCGCCTGCAACATCAGCGTTA	AGCTCGGAGGTCCCACTTTTCCT
EP3	CGCACAGCAACCTGTCAAGTA	CCCCACTAAGTCGGTGGAGC
EP4	GTGGTGCTCATCTGCTCCATTCC	AGGATGGGGTTCACAGAAGCAAT
EP3la	GGATCATGTGTGTGGTGTCC	GCAGAACTTCCGAAGAAGGA
EP3lb	TGAACAACCTGAAGTGGACTTTC	ATTCTCAGACCCAGGGAAACAGG
EP3lc	TTCGCTGAACCAGATCTTGGATC	TAGACAATGAGATGGCCTGCCCT
EP3-2	GGATCATGTGTGTGGTGTCC	GCAGAACTTCCGAAGAAGGA
EP3-3	TGAACAACCTGAAGTGGACTTTC	ATTCTCAGACCCAGGGAAACAGG
EP3-4	TTCGCTGAACCAGATCTTGGATC	TAGACAATGAGATGGCCTGCCCT
EP3-5	GGATCATGTGTGTGGTGTCC	GCAGAACTTCCGAAGAAGGA
EP3-6	TGAACAACCTGAAGTGGACTTTC	ATTCTCAGACCCAGGGAAACAGG
EP3e	TTCGCTGAACCAGATCTTGGATC	TAGACAATGAGATGGCCTGCCCT
EP3f	TTCGCTGAACCAGATCTTGGATC	TAGACAATGAGATGGCCTGCCCT
GAPDH	CCCTTATTGACCTCAACTACATGGT	GAGGGGCCATCCACAGTCTTCTG

Supplementary Table 3.

siRNA sequences

siRNA	Sense	Anti-sense
si*EP3*-1(m)	GGUCGCCGCUAUUGAUAAUTT	AUUAUCAAUAGCGGCGACCTT
si*EP3*-2(m)	GGAGUGCAAUUCCUUUCUATT	UAGAAAGGAAUUGCACUCCTT
si*EP3*-3(m)	GAGCAAUGCAAGACACAGATT	UCUGUGUCUUGCAUUGCUCTT
si*EP3A*	GACCACACCAACUAUGCUUTT	AAGCAUAGUUGGUGUGGUCTT
si*EP3B*	GGGUCUGAGAAUUUCUUCUTT	AGAAGAAAUUCUCAGACCCTT
si*EP3G*	GCUCUAGUGAUGGACAGAATT	UUCUGUCCAUCACUAGAGCTT
si*EP3*-1(h)	CUCCGCUCCUGAUAAUGAUTT	AUCAUUAUCAGGAGCGGAGTT
si*EP3*-2(h)	GCUUCACUGAACCAGAUCUTT	AGAUCUGGUUCAGUGAAGCTT
si*EP3*-3(h)	GCUGUUAAGAAAGAUCCUUTT	AAGGAUCUUUCUUAACAGCTT

m,mouse; h,human

Supplemental Figure 1

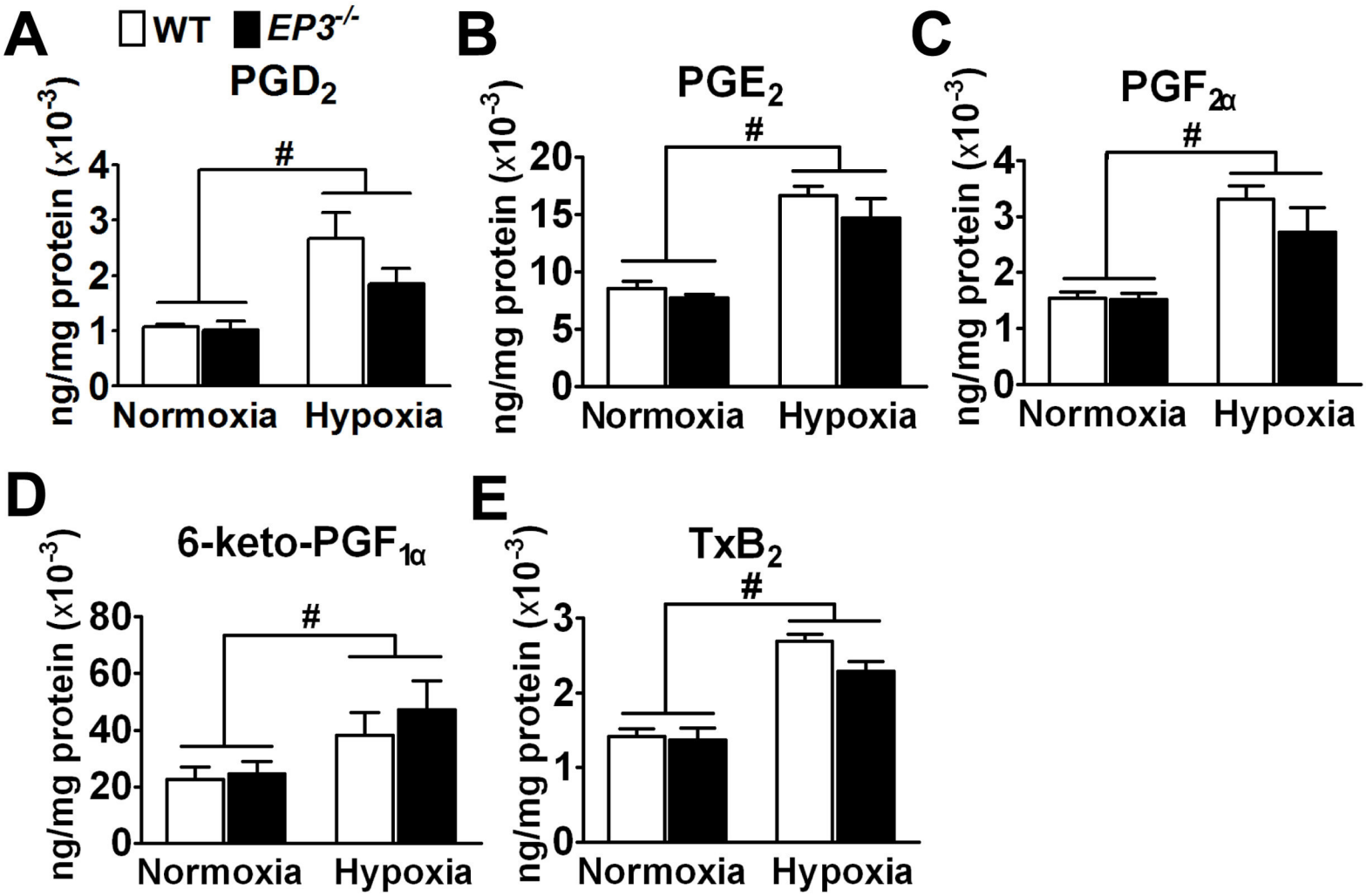

Supplemental Figure 1: Effect of hypoxia on PG profile in lungs from WT and *EP3*$^{-/-}$ mice.

Mice were exposed to 10% oxygen for 3 weeks, and then lung tissues were collected for PG extraction. PGD_2 **(A)**, PGE_2 **(B)**, $PGF_{2\alpha}$ **(C)**, 6-keto-$PGF_{1\alpha}$, a stable hydrolyzed product of PGI_2 **(D)** and TxB_2 **(E)** were detected by LC/MS/MS. Data were normalized to total protein level. n=10; $^{\#}P<0.05$ versus normoxia as indicated, 2-way ANOVA with Bonferroni post-hoc analysis.

Supplemental Figure 2

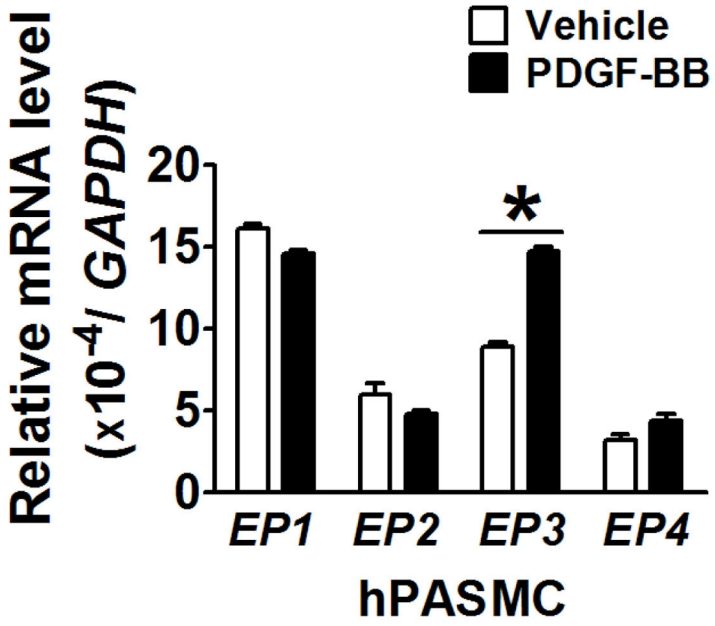

Supplemental Figure 2: *EP3* expression in PDGF-BB-treated hPASMCs.

Relative mRNA levels of *EP1–4* in PDGF-BB-treated hPASMCs. n=6, *P<0.05 versus vehicle, 2-tailed Student's *t* test.

Supplemental Figure 3

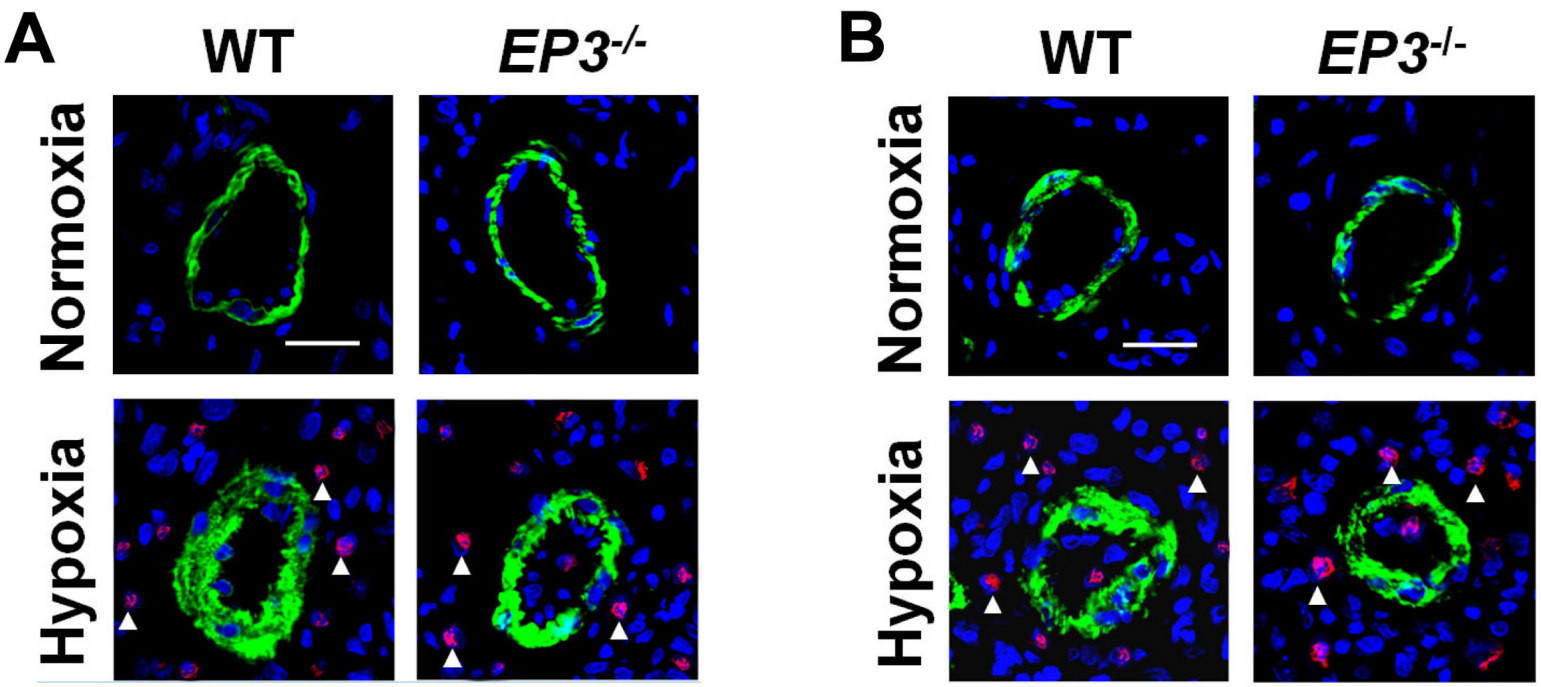

Supplemental Figure 3: Effect of *EP3* deficiency on perivascular inflammatory responses in lungs from mice with hypoxia-induced PAH.

Immunostaining of CD11b **(A**, red**)** and CD68 **(B**, red**)** of lungs from normoxia- or hypoxia-treated mice. White arrows, positive staining. Smooth muscle α-actin (SMA), green. DAPI, blue. Bar scale, 20 μm.

Supplemental Figure 4

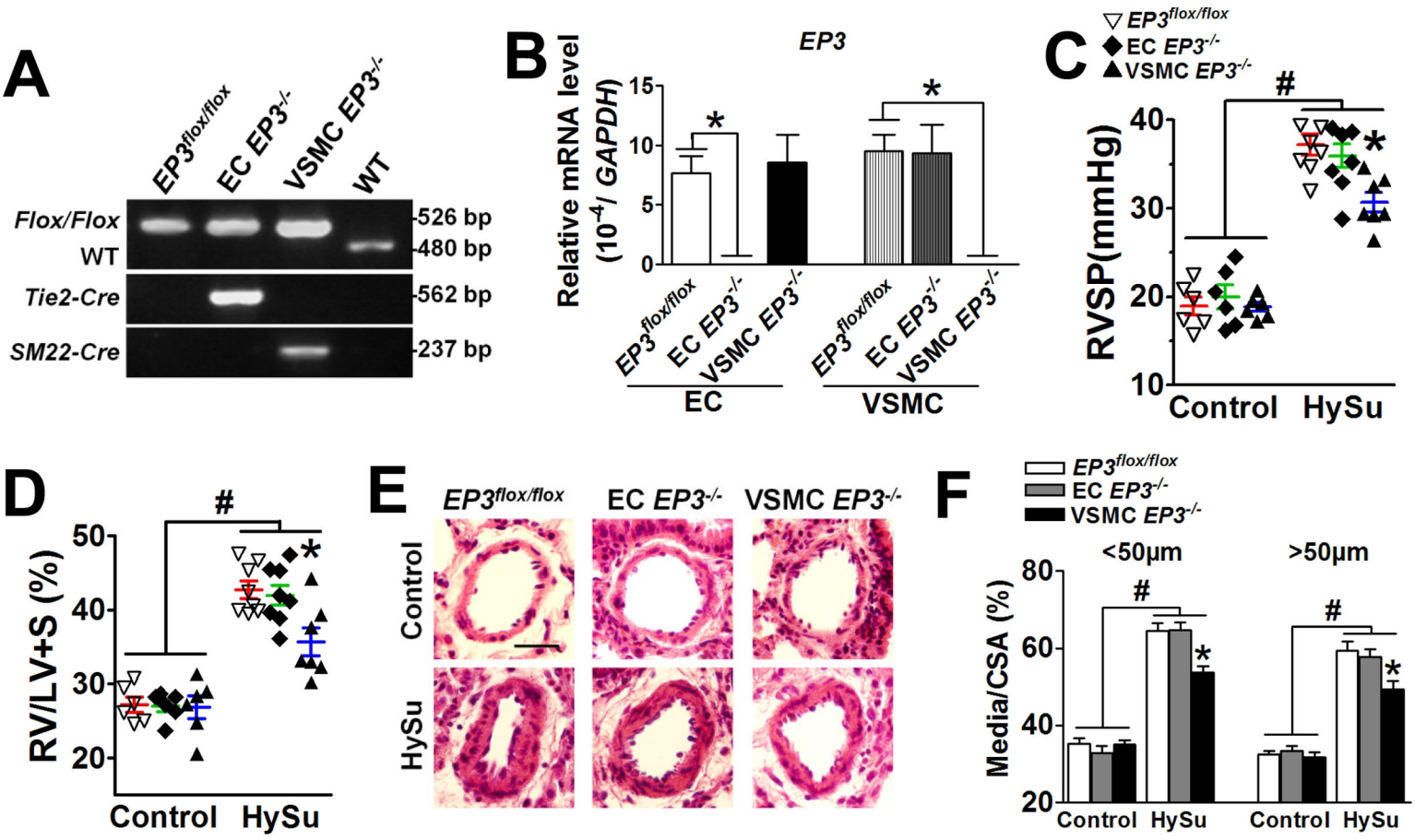

Supplemental Figure 4: *EP3* deficiency in VSMC, not in EC, attenuates pulmonary hypertension and pulmonary vascular remodeling in HySu-induced PAH in mice.

(A) Genotyping of EC- and VSMC-specific *EP3* knockout mice by PCR of genomic DNA extracted from tail biopsies. **(B)** Relative mRNA levels of *EP3* in ECs and VSMCs from EC *EP3*$^{-/-}$ and VSMC *EP3*$^{-/-}$ mice. n=4, *P<0.05, 1-way ANOVA with Bonferroni post-hoc analysis. **(C)** RVSP in EC *EP3*$^{-/-}$, VSMC *EP3*$^{-/-}$ and *EP3*$^{flox/flox}$ controls after HySu treatment. **(D)** Ratio of RV/LV+S in EC *EP3*$^{-/-}$, VSMC *EP3*$^{-/-}$ and *EP3*$^{flox/flox}$ controls after HySu treatment. **(E)** Representative images of H&E staining of pulmonary arteries. Bar scale, 20μm. **(F)** Quantification of vascular medial thickness as a ratio of total vessel size (Media/CSA) for HySu model. n=6-8 mice/group for C-F; *P<0.05 versus *EP3*$^{flox/flox}$; $^{\#}$P<0.05 versus control, 2-way ANOVA with Bonferroni post-hoc analysis.

Supplemental Figure 5

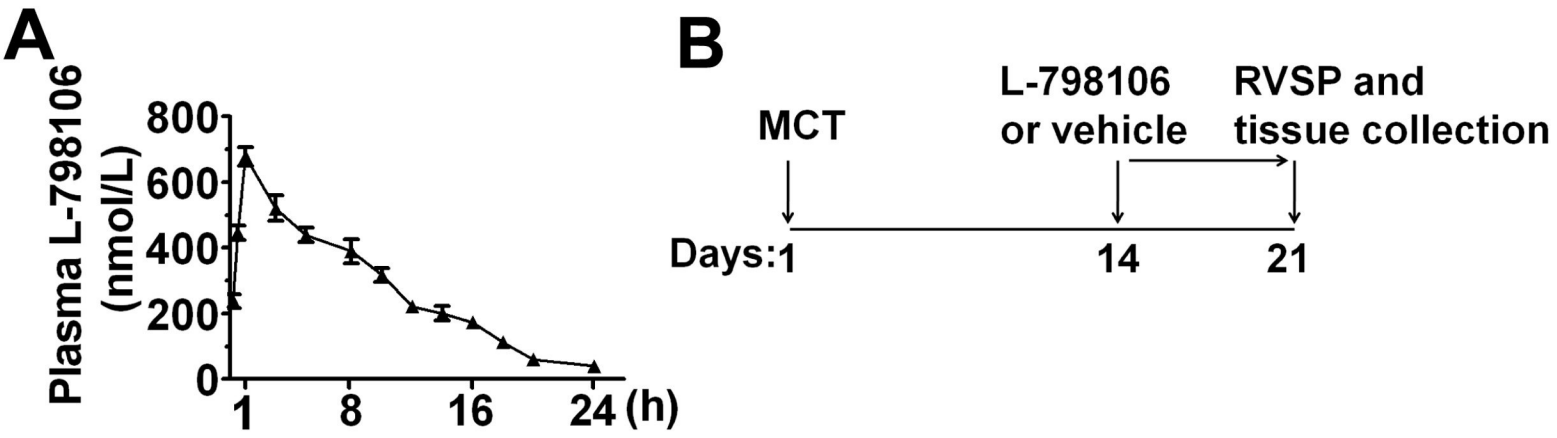

Supplemental Figure 5: Protocol for administration of L-798106 to MCT-treated rats. **(A)** Pharmacological dynamic kinetics of the EP3 inhibitor L-798106 in rats. Male, 8 week-old, Sprague-Dawley rats received intraperitoneal injection with a single dose of L-798106 (400 mg/kg), n=4. **(B)** Schematic protocol for administration of L-798106 to MCT-treated rats.

Supplemental Figure 6

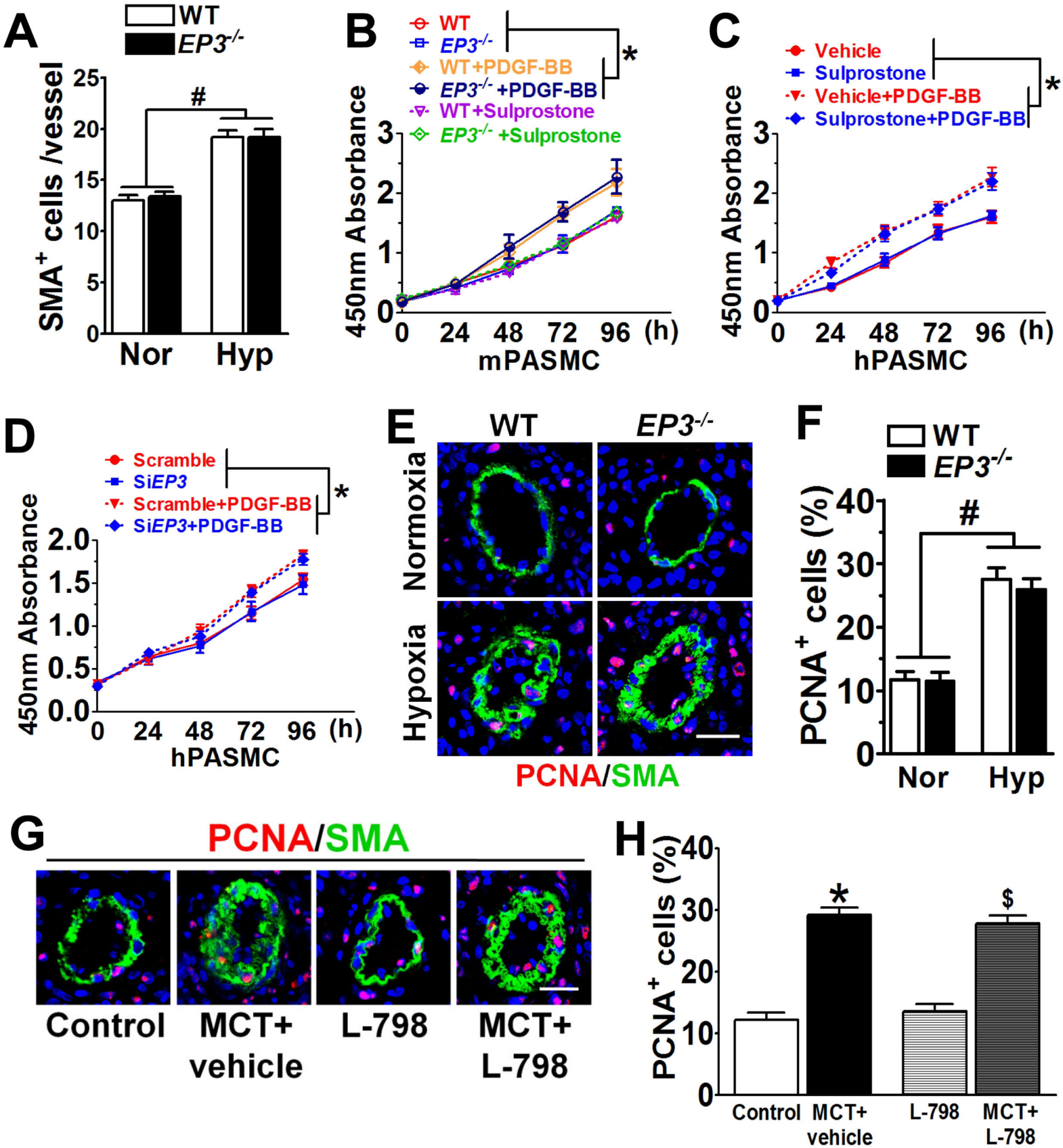

Supplemental Figure 6: Effect of genetic deletion or inhibition of EP3 on proliferation of PASMCs in vitro and in vivo.

(A) Quantification of vascular α-SMA$^+$ cells in PAs from hypoxia-induced PAH animals. At least 10 fields /mouse and 4 vessels (50-100μm) /field were selected for calculation. n=6 mice, $^{\#}$P<0.05 versus normoxia, 2-way ANOVA with Bonferroni post-hoc analysis. **(B)** Effect of *EP3* deletion on the proliferation of mPASMCs treated with PDGF-BB and sulprostone. **(C)** Effect of sulprostone on the proliferation of hPASMCs. **(D)** Effect of *EP3* knockdown on the proliferation of hPASMCs. n=4 per group for B-D; *P<0.05 as indicated, 2-way ANOVA with Bonferroni post-hoc analysis. **(E)** Representative immunostaining of PCNA (red) in lungs from hypoxia-induced PAH mice. **(F)** Quantification of vascular PCNA$^+$ cells for (E). The percentage of PCNA$^+$ cells was expressed as vascular PCNA$^+$ cells /α-SMA$^+$ cells. At least 10 fields /animal and 4 vessels (50-100μm)/field were selected for calculation. n=6 mice, $^{\#}$P<0.05 versus normoxia, 2-way ANOVA with Bonferroni post-hoc analysis. **(G)** Representative immunostaining of PCNA (red) in lungs from MCT-induced PAH rats. **(H)** Quantification of vascular PCNA$^+$ cells for (G). L-798, L-798106. n=5 rats/group, *P<0.05 versus control; $^{\$}$P <0.05 versus L-798, 2-way ANOVA with Bonferroni post-hoc analysis.

Supplemental Figure 7

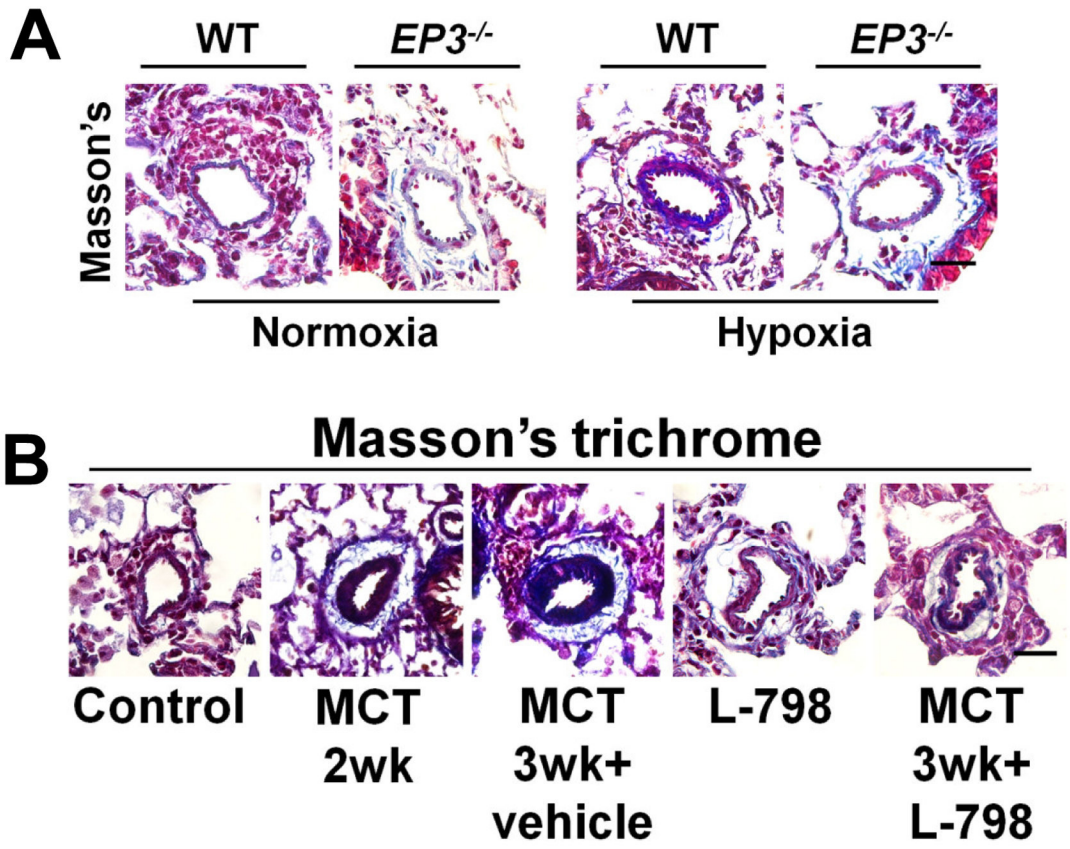

Supplemental Figure 7: Masson's trichrome staining of PAs from hypoxia-induced PAH mice (A), and MCT-treated rats (B). Mice were under exposure of chronic hypoxia (10% O_2) for 3 weeks. A dose of 200mg/kg L-798 (L-798,106) was administered to the MCT-treated rats twice per day at the beginning of the third week after MCT treatment .

Supplemental Figure 8

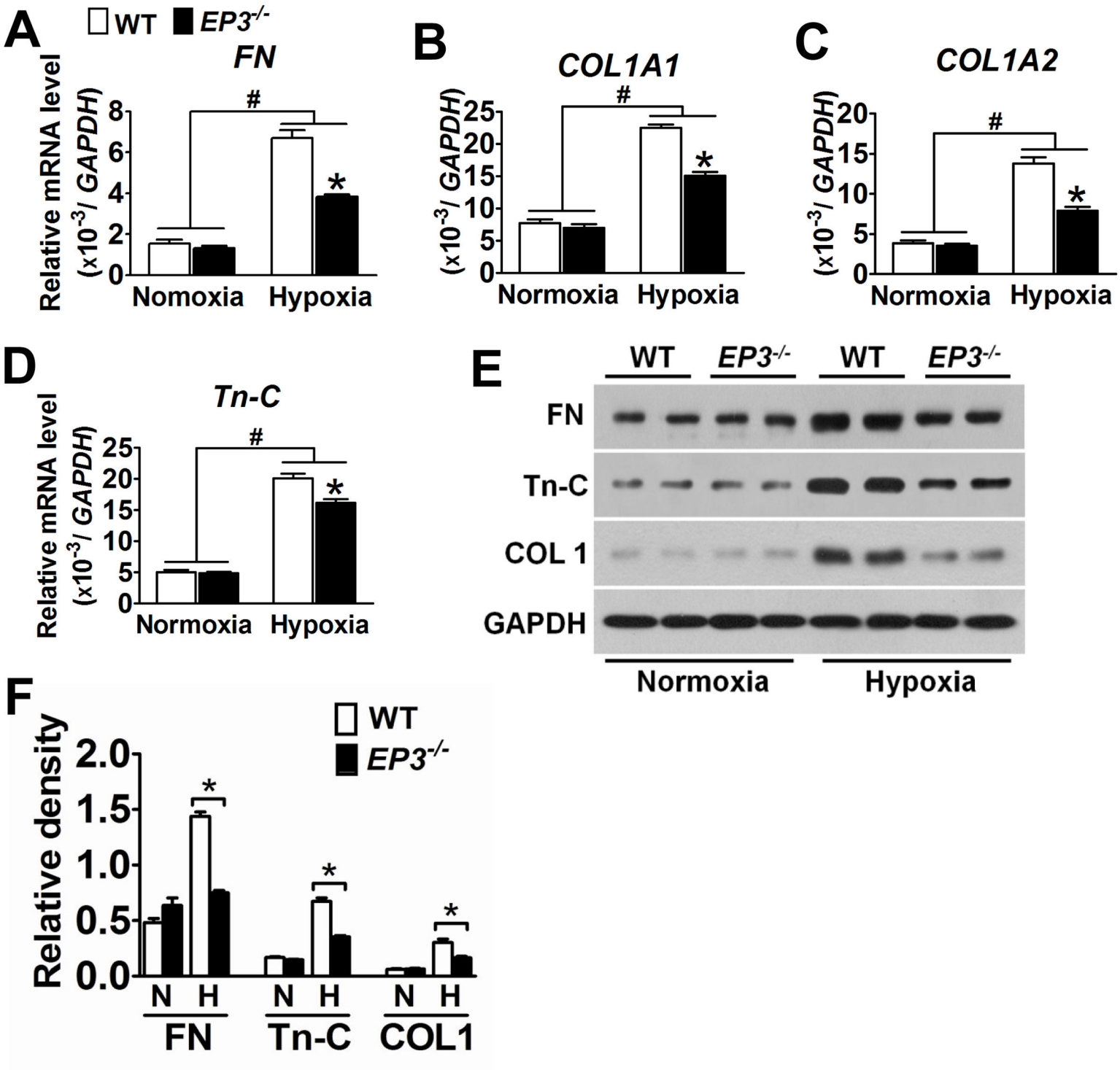

Supplemental Figure 8: Expression of the extracellular matrix protein are reduced in *EP3* deficient mPASMCs in response to hypoxia.

Effect of *EP3* deficiency on mRNA expression of fibronectin (*FN*) **(A)**, collagen 1α1 (*COL1A1*) **(B)**, collagen 1α2 (*COL1A2*) **(C)**, and tenascin-C (*Tn-C*) **(D)** in hypoxia-treated PASMCs. n=6, *P<0.05 versus WT, and #P<0.05 versus normoxia. **(E)** Western blot analysis of fibronectin, tenascin-C, and collagen 1 in hypoxia-treated mPASMCs. **(F)** Densitometric quantification of fibronectin, tenascin-C, and collagen 1 in (F). N, Normoxia; H, Hypoxia. n=6., *P<0.05 versus WT, 2-way ANOVA with Bonferroni post-hoc analysis.

Supplemental Figure 9

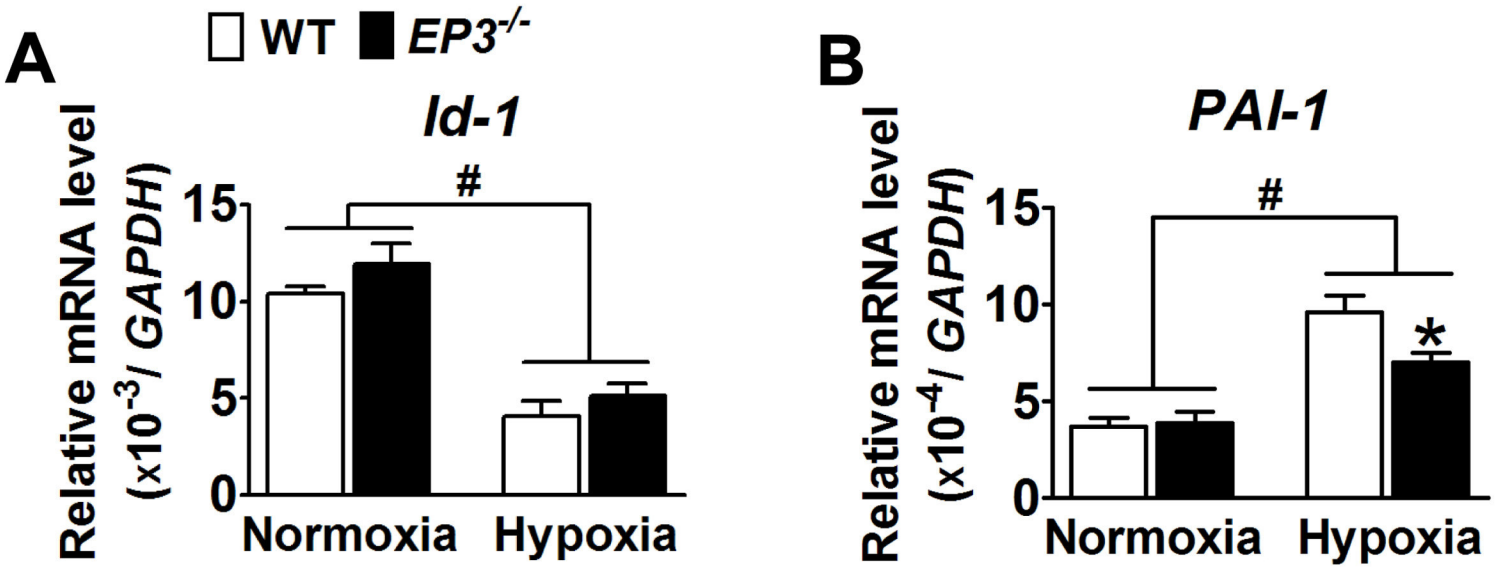

Supplemental Figure 9: *EP3* deficiency suppresses TGFβ1-targeted gene *PAI-1* but not *Id-1* in PASMCs exposed to hypoxia.

(A) Effect of *EP3* deletion on *Id-1* expression in mPASMCs exposed to hypoxia. $^{\#}P<0.05$ versus normoxia, n=6. **(B)** Effect of *EP3* deletion on *PAI-1* expression in mPASMCs exposed to hypoxia. n=6, $^{\#}P<0.05$ versus normoxia, $^{*}P<0.05$ versus WT, 2-way ANOVA with Bonferroni post-hoc analysis.

Supplemental Figure 10

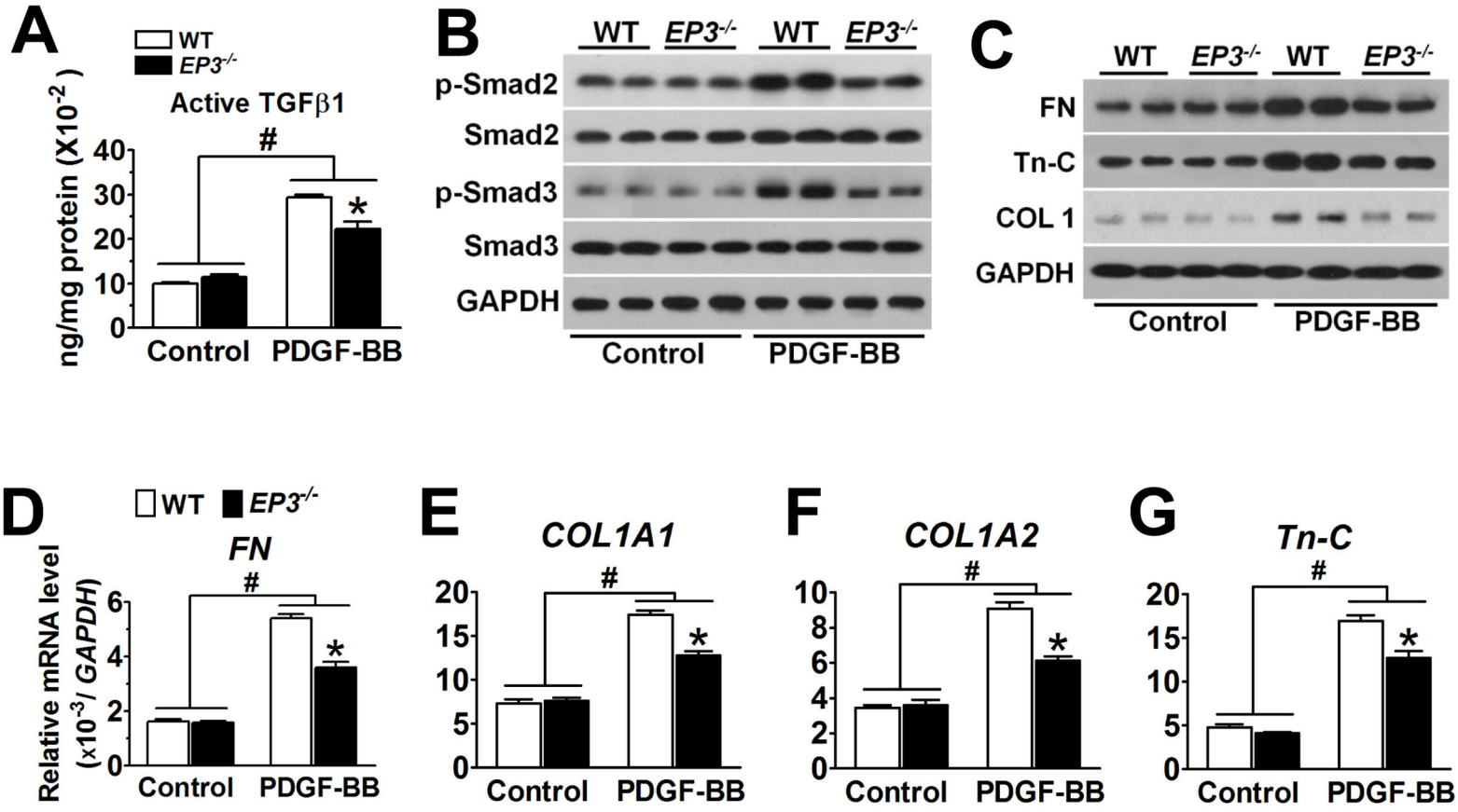

Supplemental Figure 10: Activation of TGFβ1 signaling induced by PDGF-BB is depressed in *EP3*-deficient mPASMCs.

(A) Effect of *EP3* deficiency on the content of active TGFβ1 in the culture medium of PDGF-BB-treated PASMCs. n=6. **(B)** Western blot analysis of phospho-Smad2, total Smad2, phospho-Smad3, total Smad3 of PDGF-BB-treated WT and *EP3*$^{-/-}$ PASMCs. **(C)** Western blot analysis of fibronectin (FN), collagen 1 (COL1), and tenascin-C (Tn-C) of PDGF-BB-treated WT and *EP3*$^{-/-}$ PASMCs. **(D–G)** Effect of *EP3* deficiency on mRNA expression of fibronectin (*FN*), collagen 1α1 (*COL1A1*), collagen 1α2 (*COL1A2*), and tenascin-C (*Tn-C*) of PDGF-BB-treated PASMCs. n=6; *P<0.05 versus WT, $^{\#}$P<0.05 versus vehicle control; 2-way ANOVA with Bonferroni post-hoc analysis.

Supplemental Figure 11

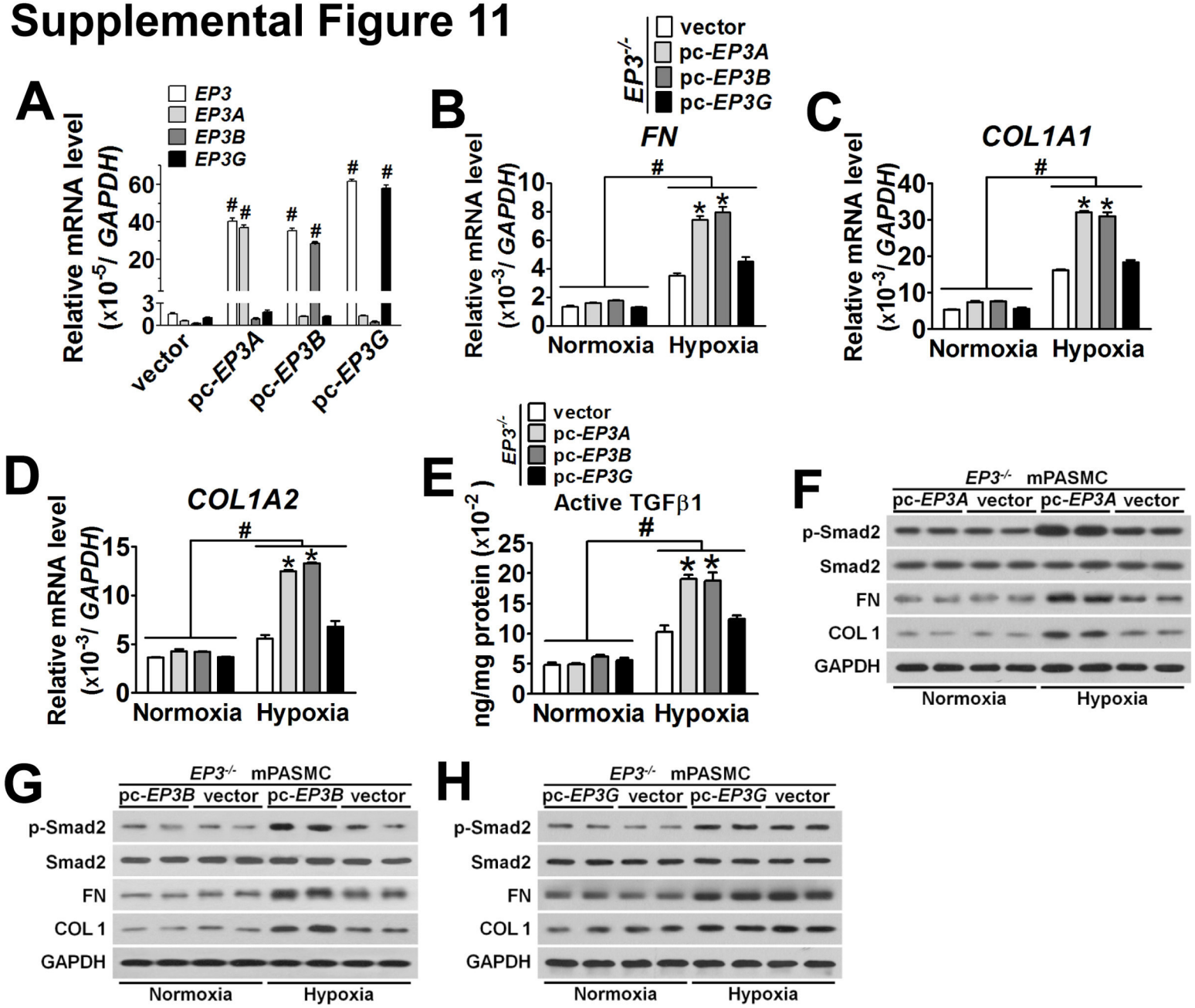

Supplemental Figure 11: Re-expression of *EP3A* and *EP3B* splice variants into *EP3*-deficient mPASMCs restores the hypoxia-induced TGFβ1 signaling.

mPASMCs from *EP3*-deficient mice were transfected with *EP3A*, *EP3B*, *EP3G* or control vector constructs, respectively. **(A)** Relative mRNA levels of *EP3* (common), *EP3A*, *EP3B*, or *EP3G* variants were analyzed by RT-PCR. n=4, #P<0.05 versus vector, 2-tailed Student *t* test. **(B–D)** Relative mRNA level of fibronectin (*FN*) **(B)**, collagen 1α1 (*COL1A1*) **(C)**, and collagen 1α2 (*COL1A2*) **(D)** were determined by RT-PCR. Data are normalized to *GAPDH* levels. **(E)** Content of active TGFβ1 in the culture medium was analyzed by ELISA. n=6; *P<0.05 versus vector and #P<0.05 versus normoxia group; 2-way ANOVA with Bonferroni post-hoc analysis. Western blot analysis of intracellular phospho-Smad2, total Smad2, FN, and COL1 proteins in mPASMCs over-expressing *EP3A* **(F)**, *EP3B* **(G),** and *EP3G* **(H)**, respectively.

Supplemental Figure 12

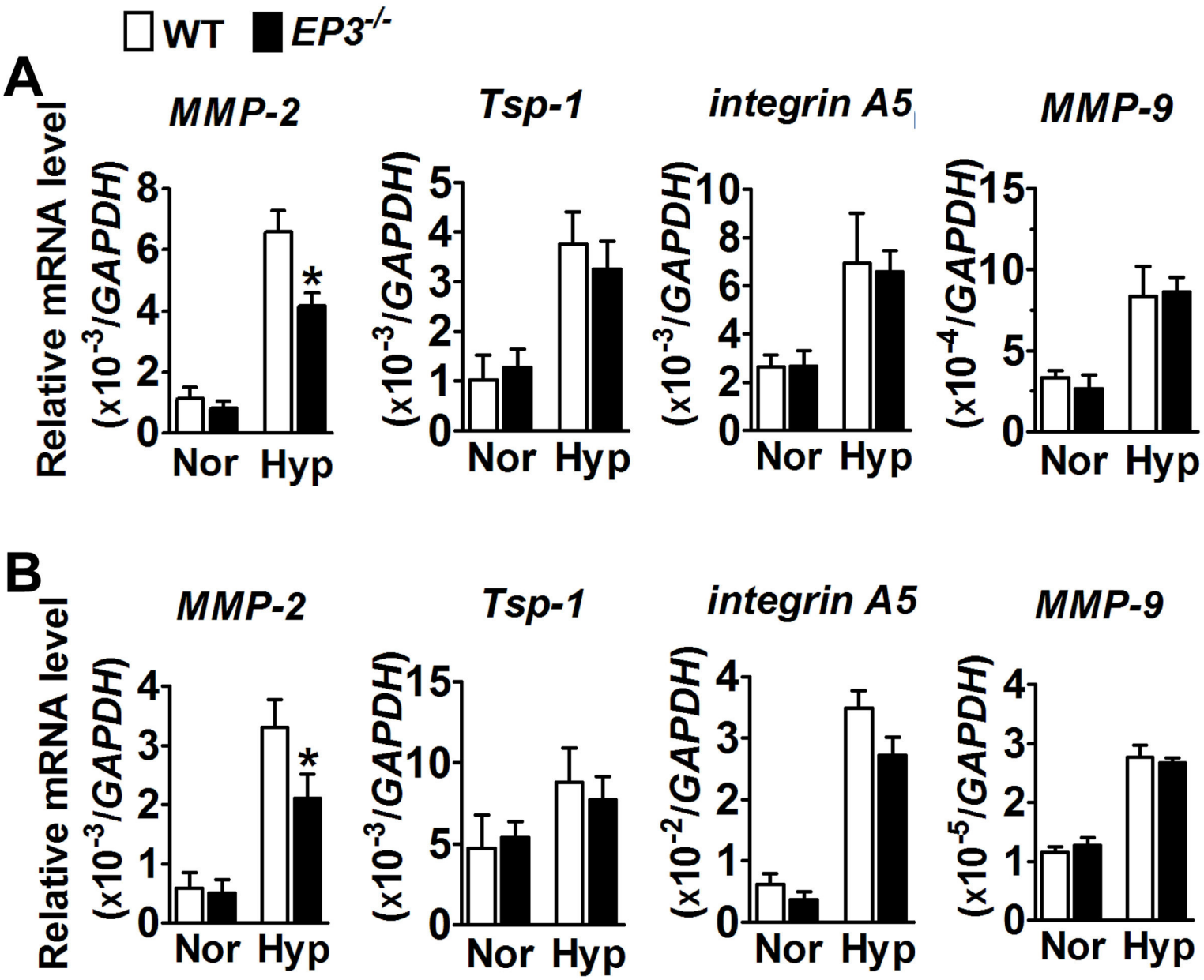

Supplemental Figure 12: *EP3* deficiency suppresses MMP-2 expression in hypoxia-treated PASMCs and lung tissues from hypoxia-induced PAH mice.

Effect of *EP3* deficiency on mRNA levels of *integrin A5*, thrombospondin-1 (*Tsp-1*), *MMP-2*, and *MMP-9* in hypoxia-treated PASMCs **(A)** and in lung tissues from hypoxia-induced PAH mice **(B)**. Nor, Normoxia; Hyp, Hypoxia. n=6; *P<0.05 versus WT, 2-tailed Student *t* test.

Supplemental Figure 13

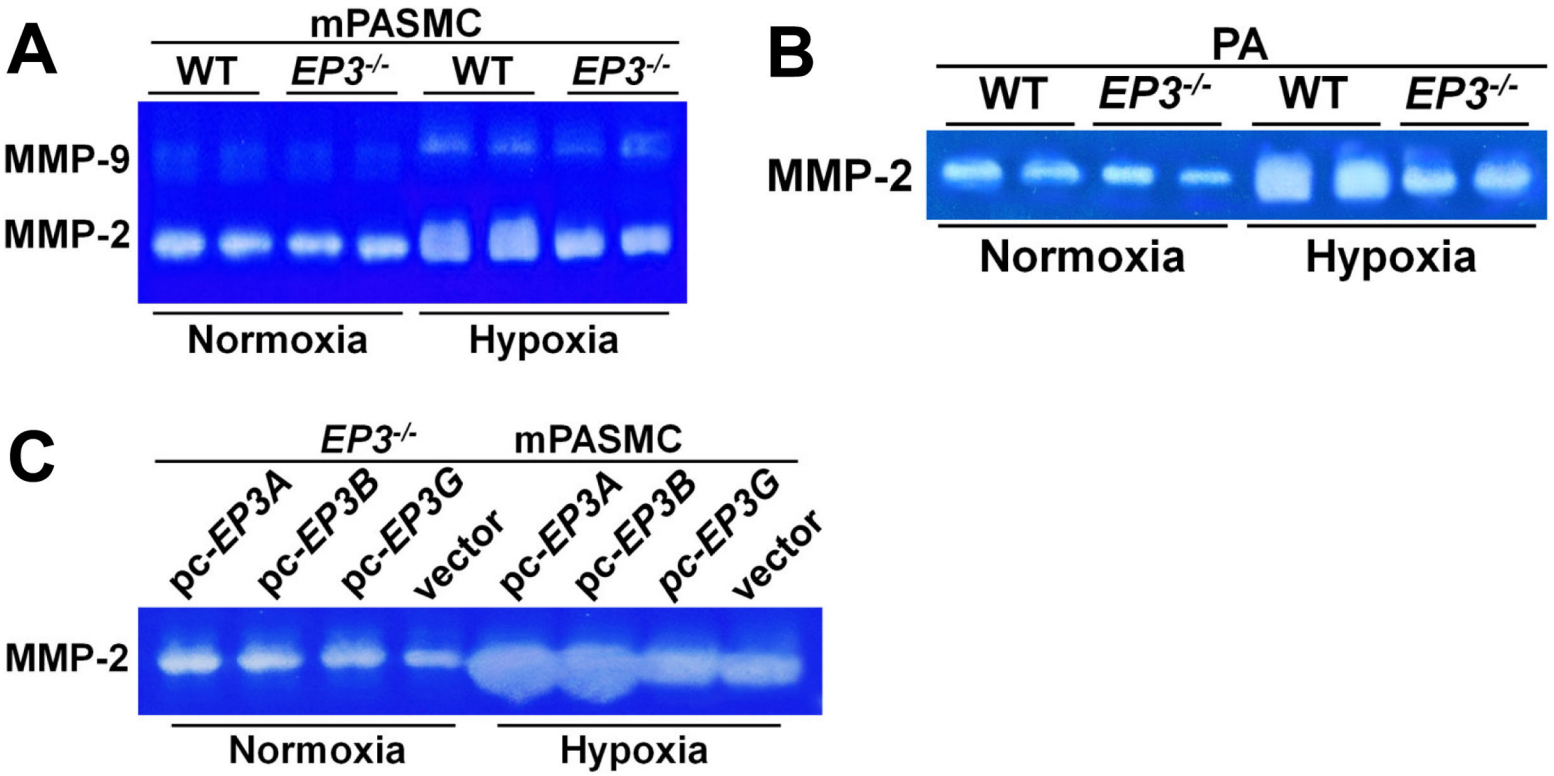

Supplemental Figure 13: *EP3A/B* variants mediate activation of extracellular MMP-2 in cultured PASMCs.

(A) Effect of *EP3* deficiency on culture MMP-2 activity of mPASMCs. **(B)** Pulmonary artery MMP-2 activity in *EP3*$^{-/-}$ and WT mice after normoxia or hypoxia treatment. **(C)** Effect of re-expressing *EP3A* or *EP3B* on culture MMP-2 activity in *EP3*-deficient PASMCs.

Supplemental Figure 14

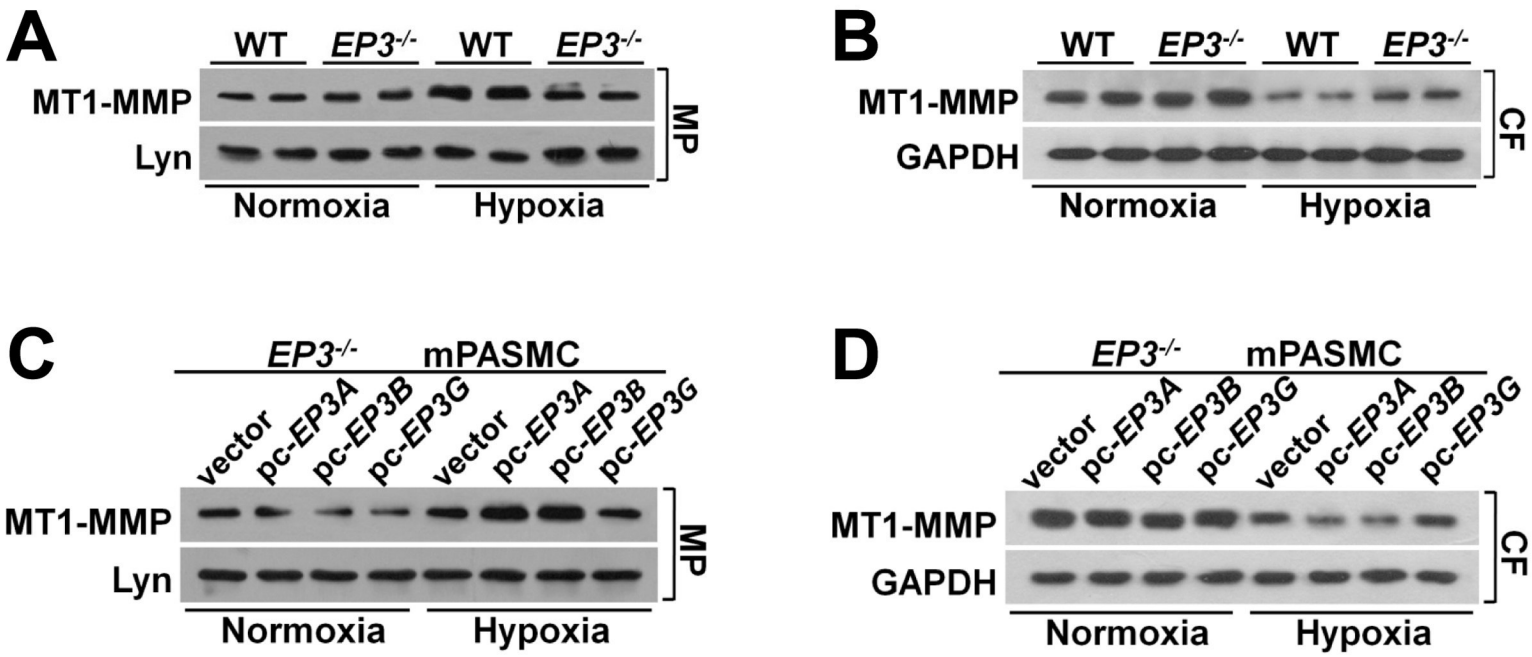

Supplemental Figure 14: *EP3A/B* variants mediate membrane localization of MT1-MMP in mPASMCs in response to hypoxia exposure.

(A-B) Effect of *EP3* deficiency on membrane localization (A) and cytoplasmic expression (B) of MT1-MMP in mPASMCs. MP, Membrane Protein. CF, Cytosol Fraction. **(C-D)** Effect of forced expression of *EP3A*, *EP3B*, or *EP3G* on membrane localization (C) and cytoplasmic expression (D) of MT1-MMP in *EP3*-deficient PASMCs. Results were repeated 2 times.

Supplemental Figure 15

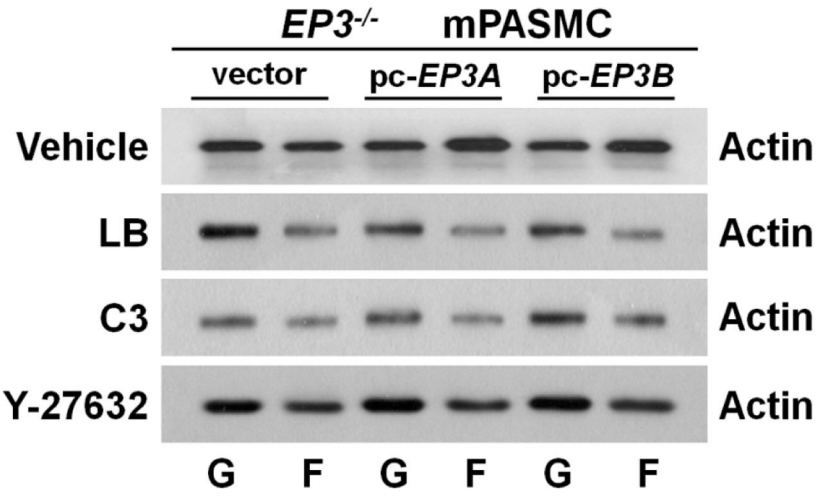

Supplemental Figure 15: Immunoblots of F- versus G-actin ratio in hypoxia-treated *EP3A/B* complemented PASMCs in the presence or absence of LB (10 nM**), C3 (**0.25 μg/ml**) , or Y-27632 (**10 μM**) .** LB, latrunculin B. C3, C3 transferase.

Supplemental Figure 16

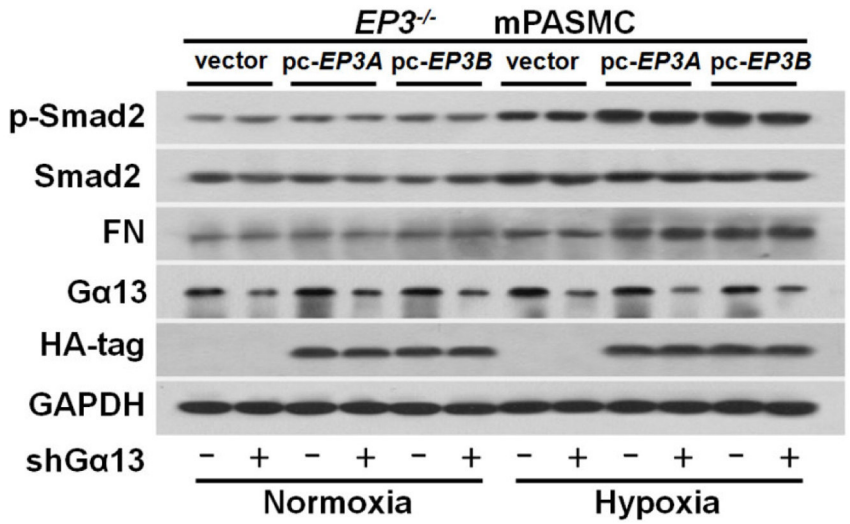

Supplemental Figure 16: Effect of knocking down $G_{\alpha 13}$ on *EP3A/B*-mediated TGFβ1 signaling in PASMCs.

Supplemental Figure 17

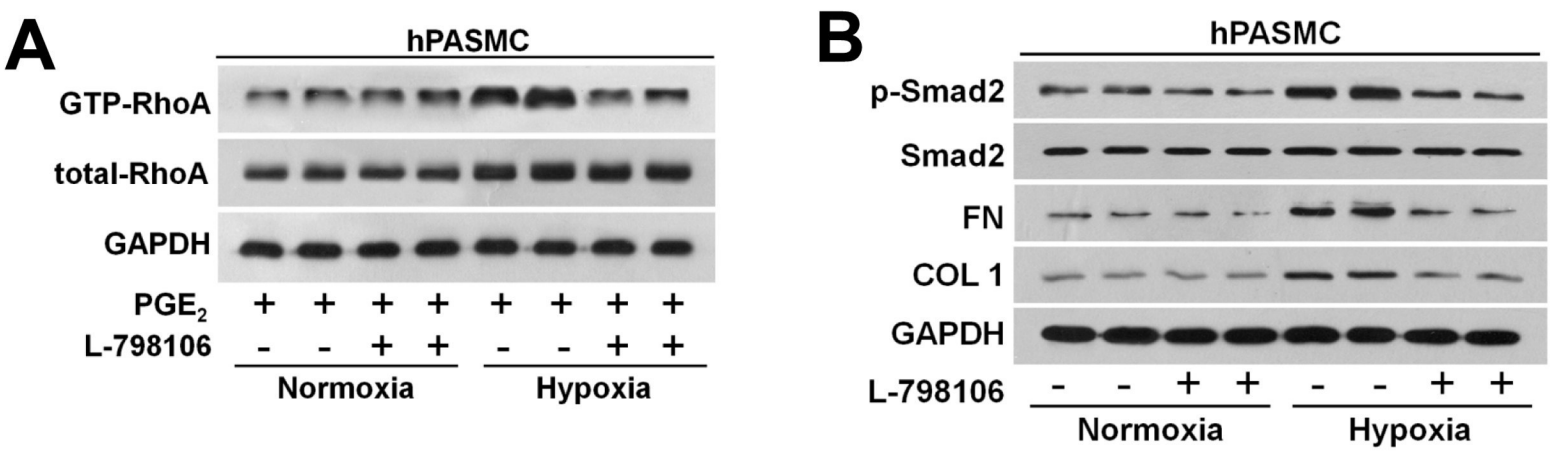

Supplemental Figure 17: EP3 antagonist decreases RhoA/ROCK dependent activation of TGFβ1 signaling in human PASMCs.

(A) Western blot analysis of active RhoA in hPASMCs treated with L-798106 (10 μM) . **(B)** Effect of L-798106 treatment (10 μM) on TGFβ1 signaling in hPASMCs.